

98-04-21 TUE
11:04:18

Recent study of the high performance confinement and the high beta plasmas on the Large Helical Devices

K.Y. Watanabe, A. Komori, H. Yamada, K. Kawahata, T. Mutoh, N. Ohyaibu, O. Kaneko, S. Imagawa, Y. Nagayama, T. Shimosuma, K. Ida, T. Mito, R. Sakamoto, S. Ohdachi, K. Nagaoka, R. Kumazawa, H. Funaba, M. Kobayashi, S. Masuzaki, O. Mitarai, Y. Narusima, S. Sakakibara, M. Sato, M. Yoshinuma, S. Sudo, O. Motojima, and LHD experimental Group

National Institute for Fusion Science, 322-6 Oroshi-cho, Toki 509-5292, Japan
a Liberal Arts Education Center, Kumamoto Campus, Tokai University, 9-1-1
Toroku, Kumamoto 862-8652, Japan

*Special Thanks the LHD technical staff
for their support of the experiments.*

Exp. started at
F.Y.1998

Shot

90426

(Up to Dec.5/2008)

Largest helical and super conducting
machine in the world

Magnetic energy 1 GJ

Cryogenic mass(-269°C) 850 t

Tolerance < 2mm

External dia. 13.5 m

Plasma Maj. R. ~3.7 m

Plasma Min. R. ~0.6 m

Plasma Vol. ~30 m³

Magnetic field 3 T

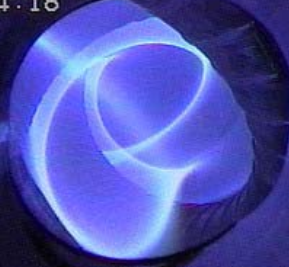
Total weight 1,500 t

ECH 77 – 168 GHz/~3MW

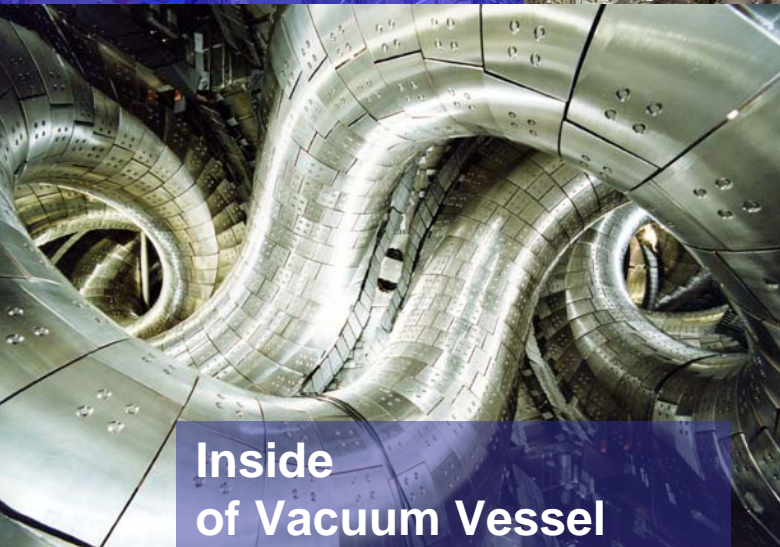
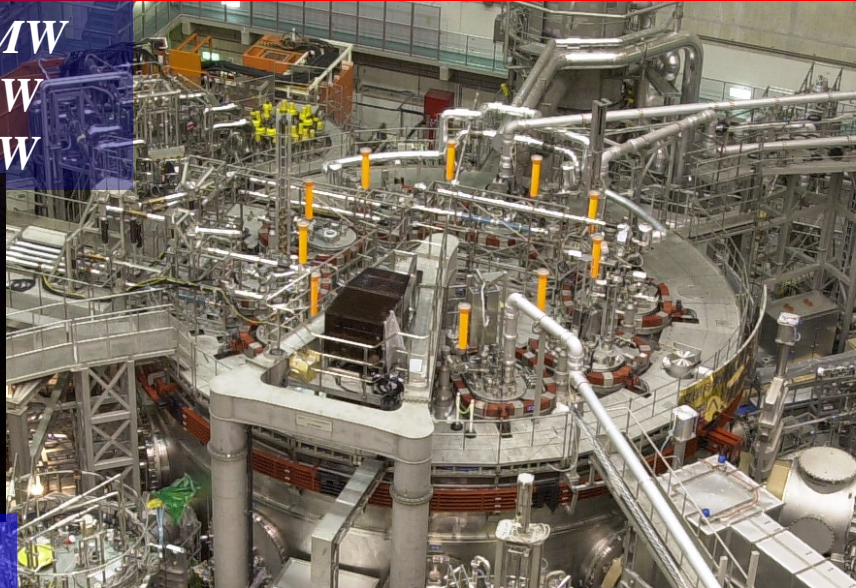
ICH 25-100 MHz/~3MW

NBI para.+perp./~23MW

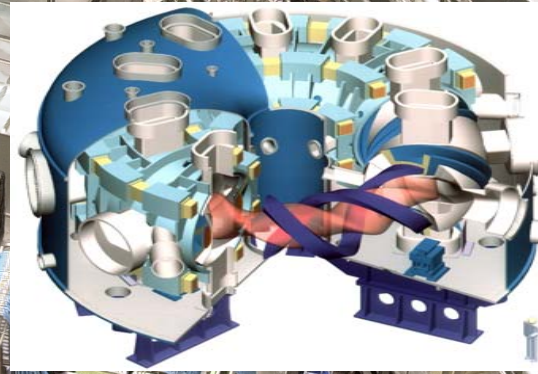
98-04-21 TUE
11:04:18



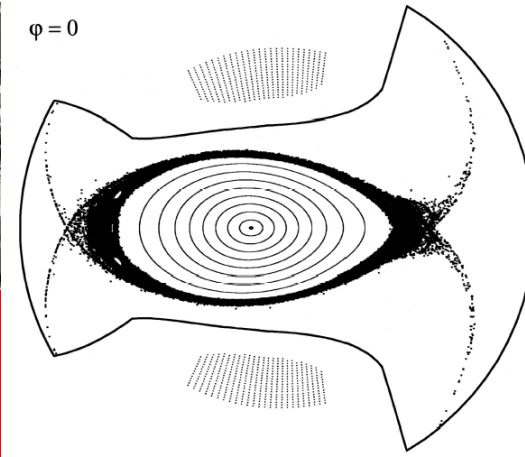
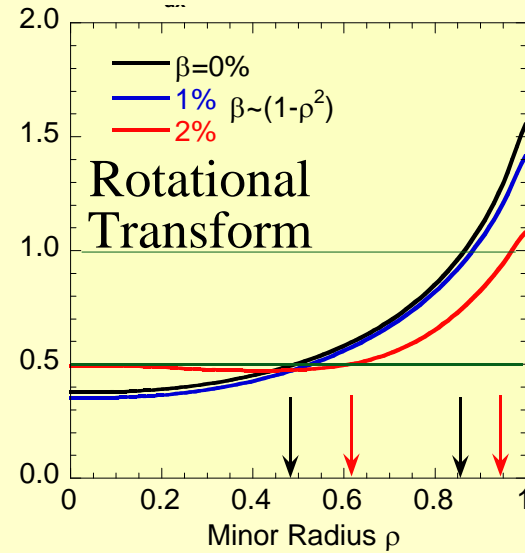
Light from plasma



Inside
of Vacuum Vessel



Large Helical Device
(LHD, NIFS, Japan)



Recent achievements and Designed target in LHD

Achievements [Designed target]

Ion Temperature

Central T_i 5.2 keV (Low Z) [10 keV]
Density $1.6 \times 10^{19} \text{m}^{-3}$ [$2 \times 10^{19} \text{m}^{-3}$]

Electron Temperature

Central T_e 10 keV [10 keV]

Density $5 \times 10^{18} \text{m}^{-3}$ [$2 \times 10^{19} \text{m}^{-3}$]

> 10 keV : reactor condition

Volume Averaged β

5.1 % transient, 5% quasi-steady
($B_0=0.425\text{T}$) [$\geq 5\%$ (1-2 T)]

Economical reactor

Steady State Operation

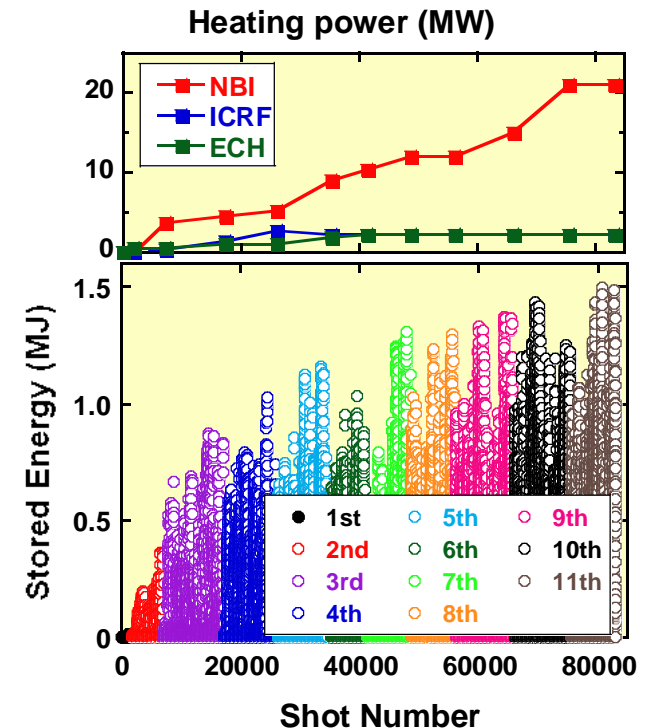
54m28s (490 kW) 1.6 GJ

800s (1.1 MW) [1 hour (3 MW)]

Largest input energy

High Density

$1.1 \times 10^{21} \text{m}^{-3}$ (Super high density with Peaked prof.)



High stored energy
comparable to big tokamaks

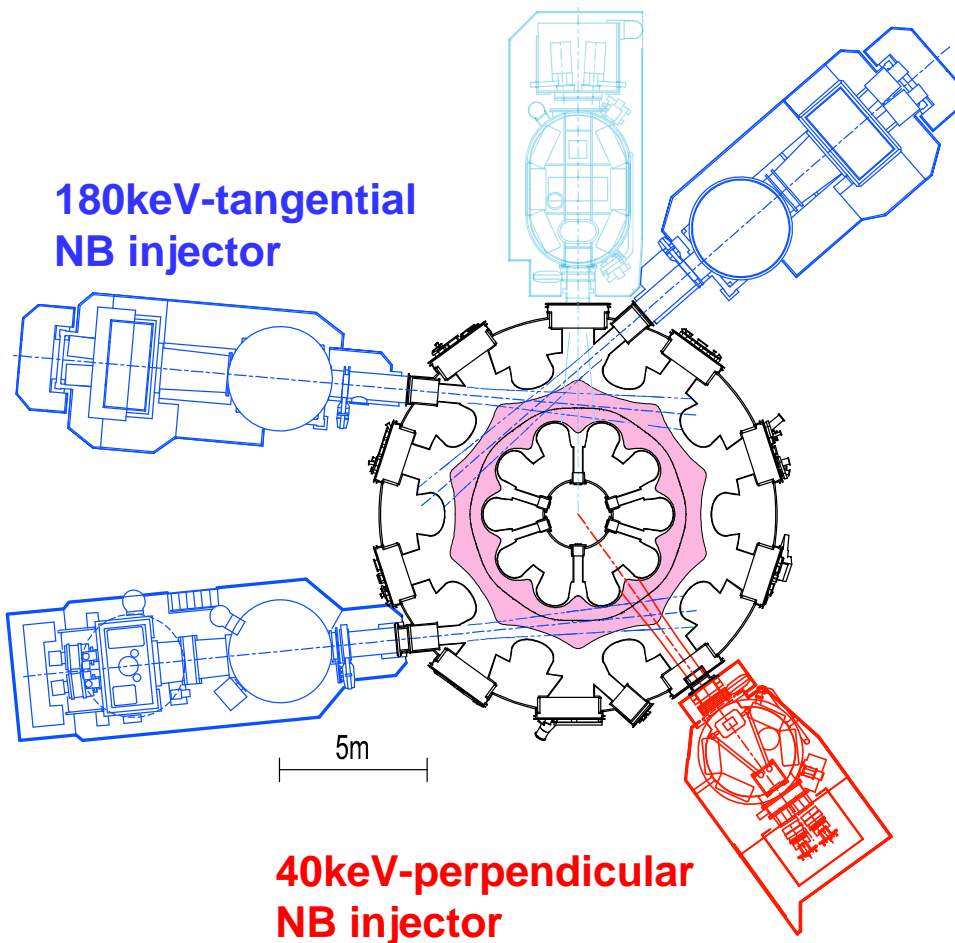
In the large plasma parameter space
systematic investigations become possible
→ *Accumulation of physical data*

Outline

1. High ion temperature with confinement improvement similar to *Internal Transport Barrier (ITB)*
2. High density $n_e(0) > 10^{21} \text{m}^{-3}$ with *Internal Diffusion Barrier (IDB)*
3. High beta $\langle \beta \rangle = 5\%$ in quasi-steady state
4. Steady state operation with high input power and high heat load
5. Summary

Update of NBI heating system to improve ion transport study

- ✓ 4 beam lines of NBI (at present)
= 3 tangential + 1 perpendicular (+ 1 perpendicular in 2010 ; *in plan*)



Tangential beams

- 16 MW in total, $E_{\text{NBI}} = 180 \text{ keV}$ with negative-ion sources
- Primarily electron heating
- Good heating efficiency

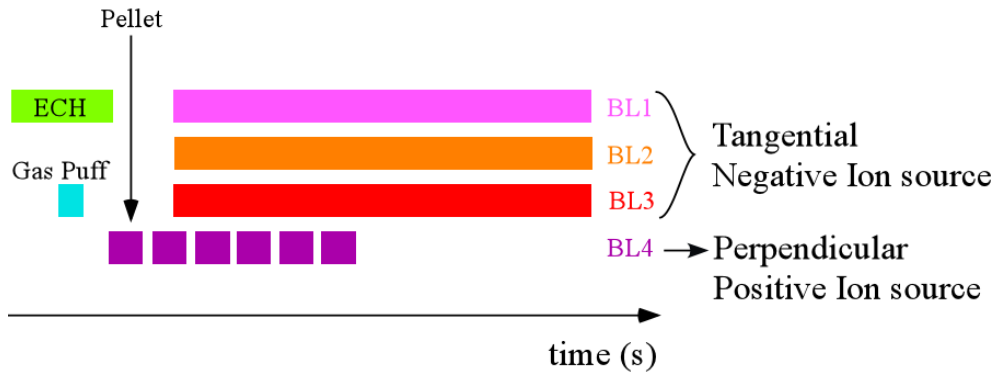
Perpendicular beam; updated

- 7 MW, $E_{\text{NBI}} = 40 \text{ keV}$ with positive-ion sources
- **Ion heating**
- works as a diagnostic beam for CXRS (T_i , V_ϕ , V_θ , E_r)

Total input power; 23 MW

Schematic view for High Ti Discharge

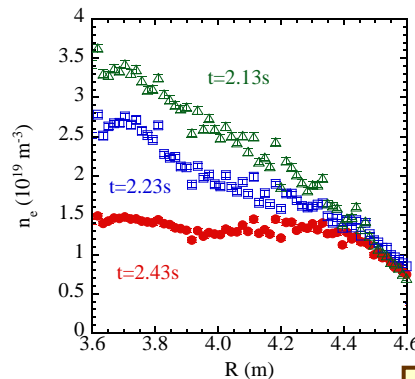
Schematic View of discharge



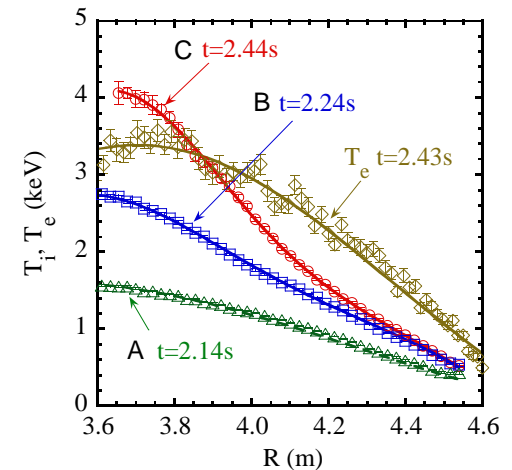
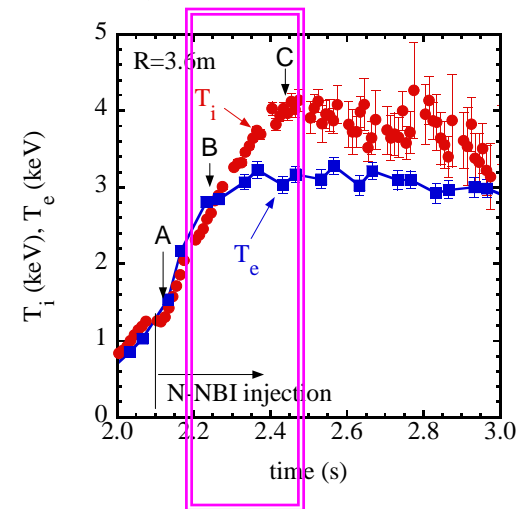
- # Plasma produced with ECH and sustained with NBI.
- # Particles are fueled with Gas puffing or pellet injection and NBI.
- # NBI with positive ion sources is modulated on and off with 5Hz for CXRS.

Typical density at high T_i phase

$$n_e = 1 \sim 2 \times 10^{19} \text{ m}^{-3}$$

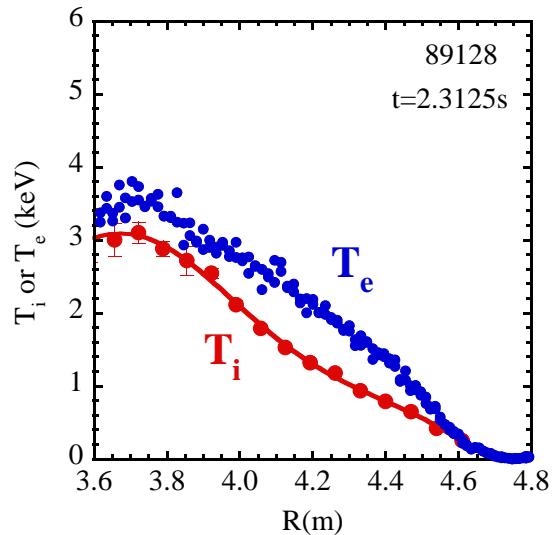


Ti, Te Time Trace



High Ti discharge with confinement improvement

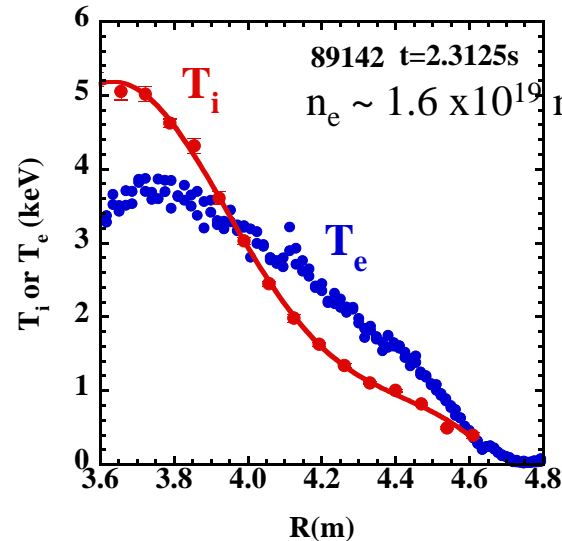
L-mode



$$T_i < T_e$$

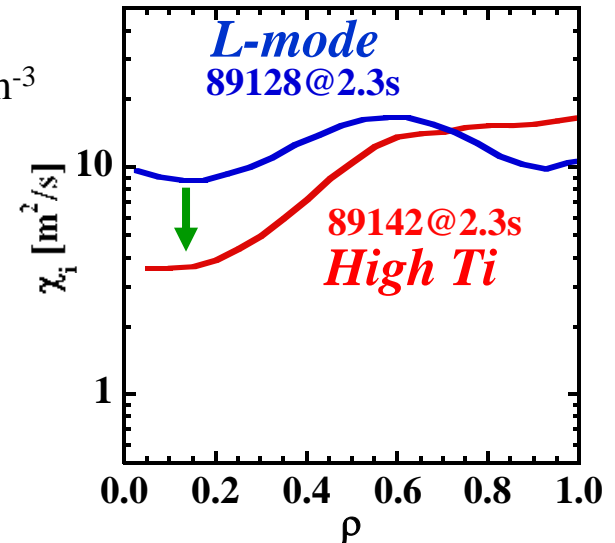
$$\nabla T_i \sim \nabla T_e \text{ at } \rho < 0.5$$

Improved confinement with
Internal Transport Barrier



$$T_i > T_e$$

$$\nabla T_i \gg \nabla T_e \text{ at } \rho < 0.5$$



Improvement of ion
transport in Core

Mechanism of the Ion ITB formation; under investigation

What is the key parameter?

Ratio of T_e/T_i , Deposition power, E_r , V_t and so on?

Extension of the high density operation regime with good energy confinement in IDB plasmas

Achievements of high n and high p in Internal Diffusion Barrier plasmas

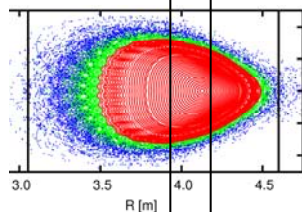
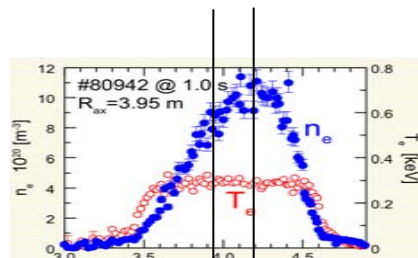
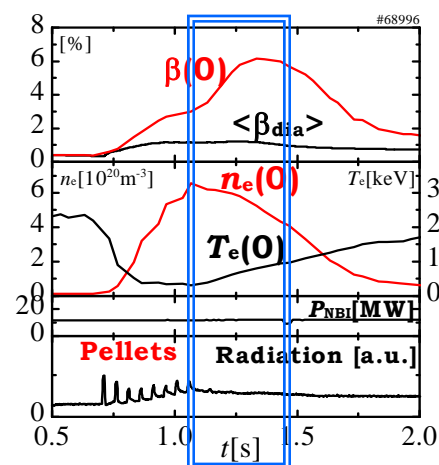
- # Super high density with peaked prof. is obtained just after the multi-pellet injection.

Maximum $n_e(0)$ exceeds $1 \times 10^{21} \text{ m}^{-3}$

- # High central pressure is obtained during the density decay phase.

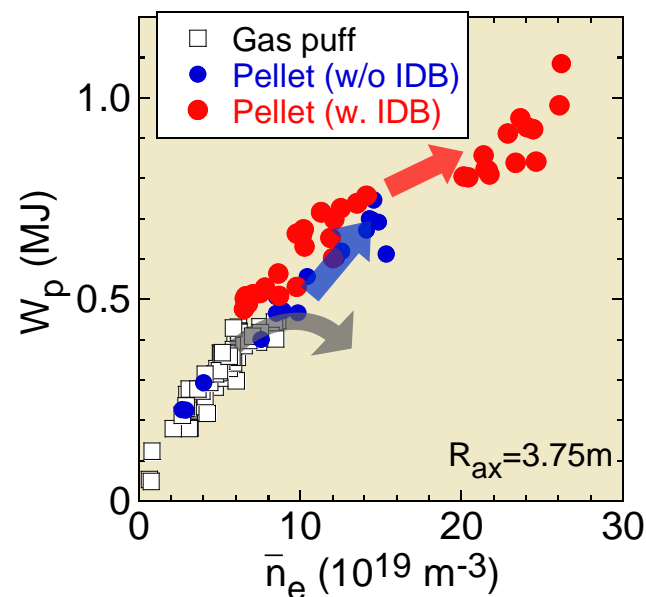
Maximum $P(0) \sim 150 \text{ kPa}$

Large Shafranov shift;
reaches to half the radius
predicts large stochastic region.



HINT

- # Confinement capability rolls over in high density regime w/o IDB
- # IDB plasmas extend the high density regimes with the good energy confinement (ISS95 scaling).



Operational limit of IDB plasmas

Limitation of central pressure by Core Density Collapse

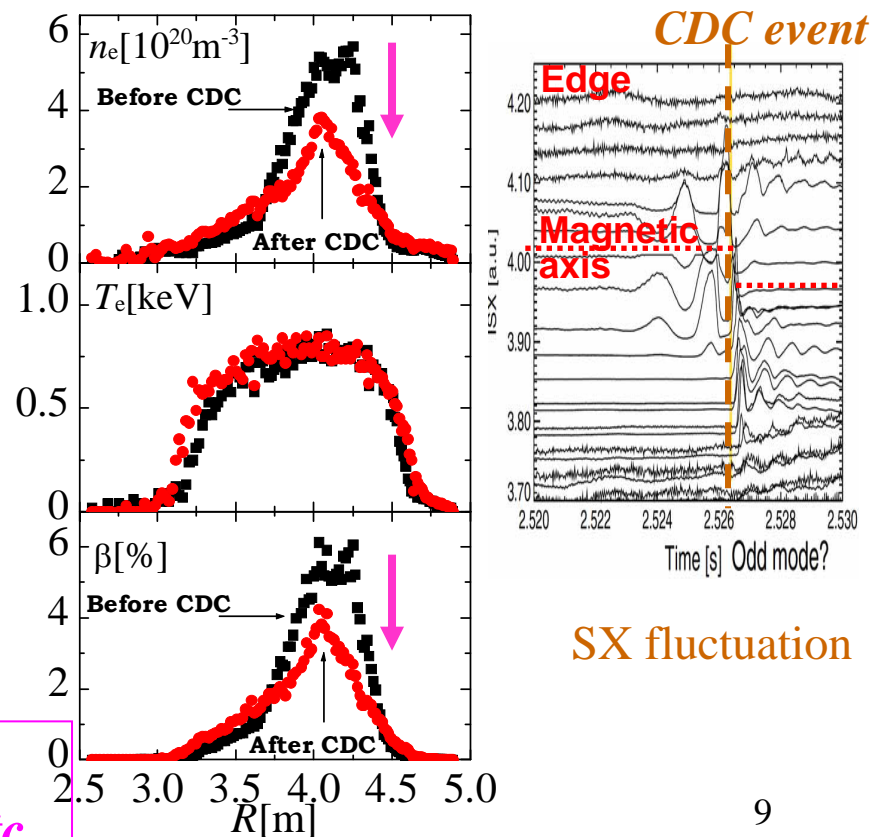
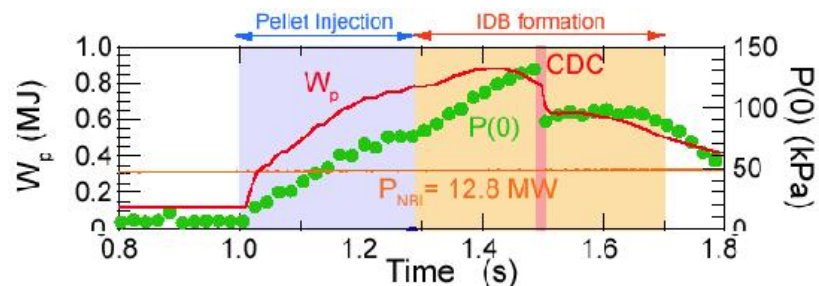
- # Core density is abruptly expelled at high central pressure phase
- # Sometimes MHD events are observed around CDC.

Driving mechanism;
under investigation
(MHD insta. and/or equil. limit)

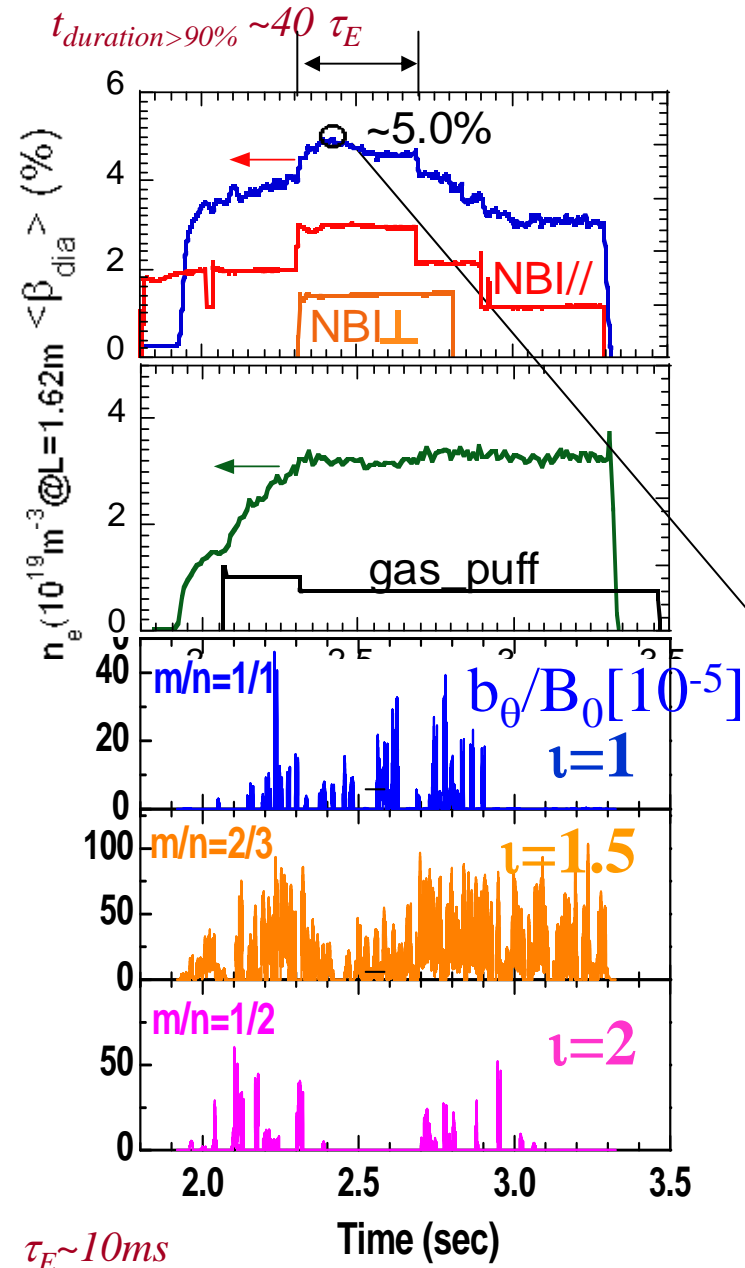
Limitation of central density by lack of central heating power

- # High density plasma inhibit NB penetration to the core
- # Density rise by pellet is limited

Central heating efficiency is a key issue
=> *high energy NBI. Bernstein Wave etc.*

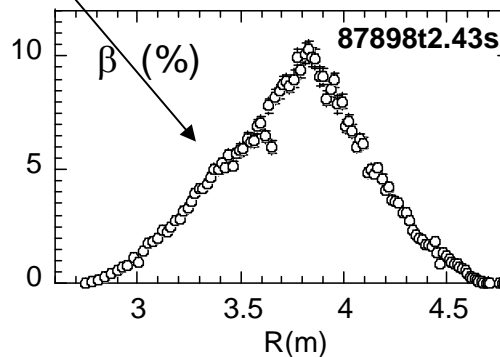


Quasi-steady high- β discharge $\langle\beta\rangle=5.0\%$



$B_0 \sim 0.425 \text{ T}$, $R \sim 3.7 \text{ m}$, $a_p \sim 0.55 \text{ m}$, $V_p \sim 22 \text{ m}^3$
 Mainly tangential NB heats plasmas

- # No disruptive high beta plasma is maintained during around $40\tau_E$
- # Large shafranov shift $\Delta/a_p \sim 40\%$
- # Low- n, m MHD activities
 - No observation of core resonant modes.
 - **Only resonating mode with peripheral surf. ($m/n = 2/3$ and $1/1$) appear**



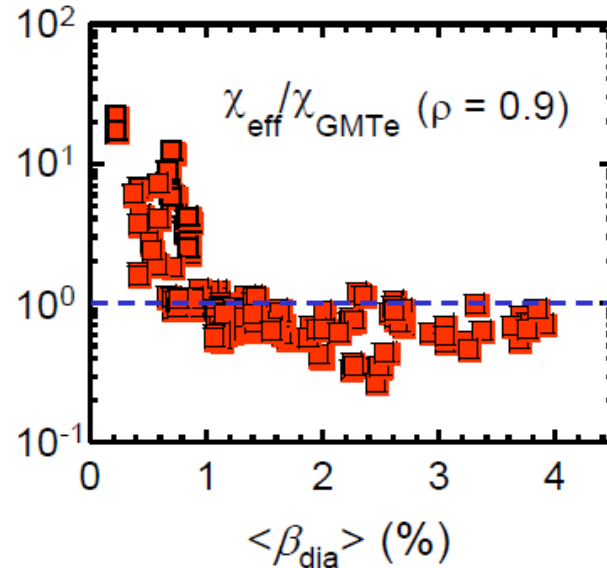
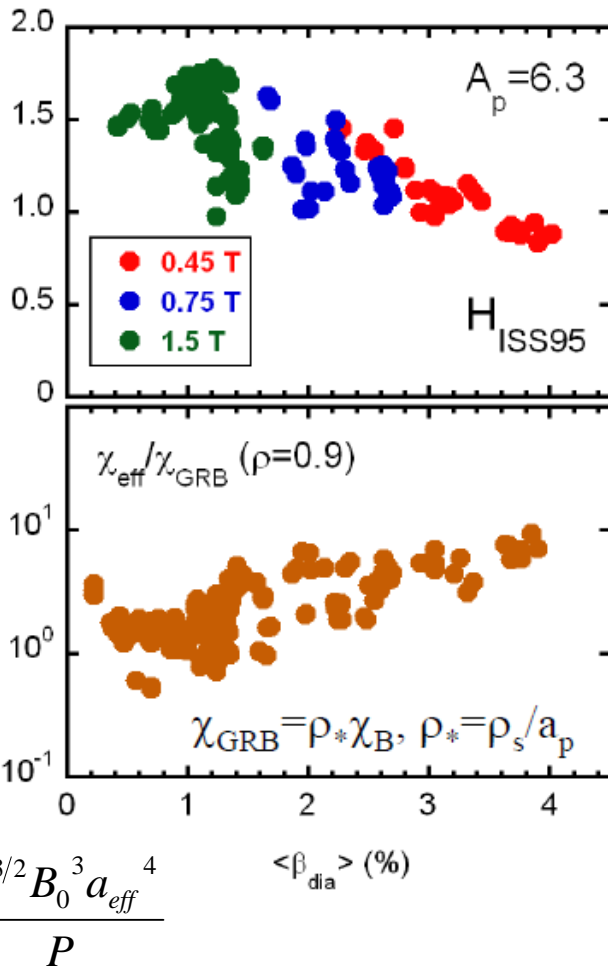
Some fine structures are observed.

Theoretically;
 Low- n MHD insta. with narrow radial mode width are predicted.

Fine structure (flattening and asymmetry) effect on a global confinement looks small

Effect of MHD instability on the confinement

Global confinement and peripheral local transport degrading with beta



χ dependence on β is similar with a prediction based on MHD (resistive interchange mode) driven turbulence.

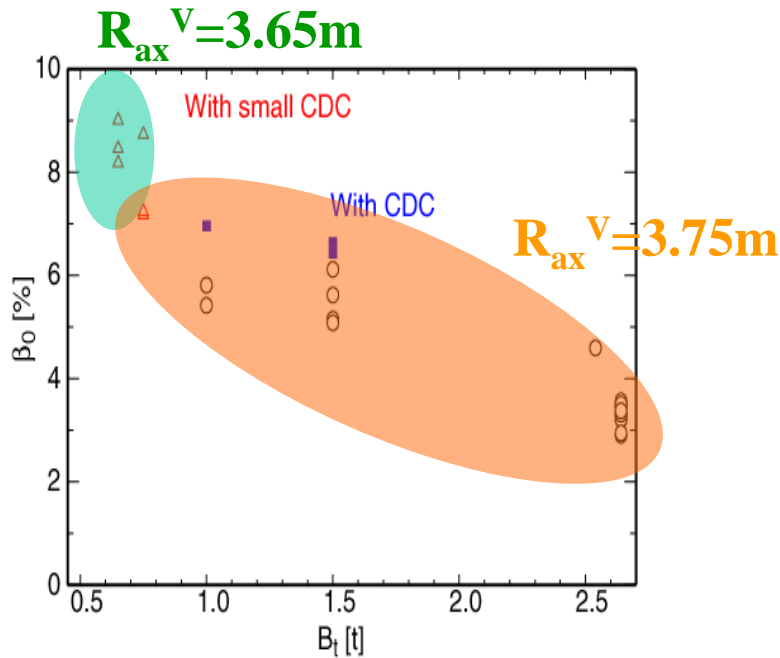
$$\chi_{GMTe} \propto \beta^1 v_{p*}^{0.67} \rho_*^{0.33} \chi_B \propto S^{-\frac{2}{3}}$$

proposed by Carreras et al. (PoF B1 (1989))

Present LHD $\langle \beta \rangle \sim 5\%$ is obtained in 0.42T, 1T, $\langle \beta \rangle \sim 4\%$ plasma $\Rightarrow S$; 10 times larger

Magnetic Reynolds number, S , is a key parameter for resistive MHD insta.

High central beta plasmas by IDB formation

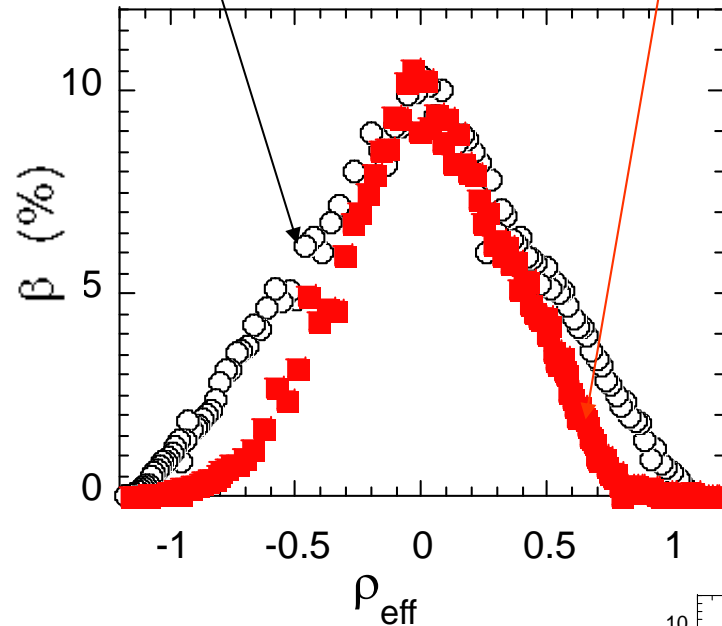


As B_t decreases,
 CDC effect on confinement
 becomes small
 \Rightarrow Achieved β_0 increases

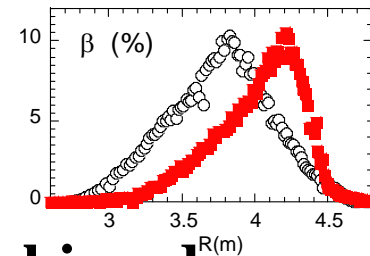
Reason not clear yet!!

Standard Scenario
 $\langle \beta \rangle \sim 5\%$

IDB Scenario
 $\langle \beta \rangle \sim 2.5\%$

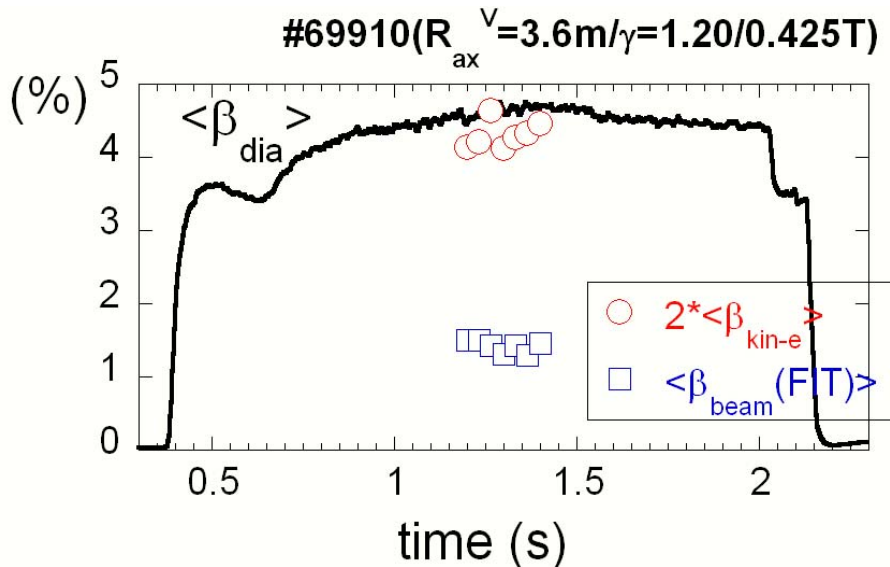


β_0 comparable with
 standard high beta
 operation has been achieved
 by IDB formation



Large beam pressure component is predicted in high β

$\langle \beta_{kin} \rangle$; 3.6% ($Z_{eff}=2.5$), $\langle \beta_{beam} \rangle$; 1.5% (Cal.)



Port-through power //NBI 13.8MW

$\langle \beta_{dia} \rangle$; 4.8% ($\beta_{perp} \sim 3.2$)

$\langle \beta_{kin} \rangle$; 3.6% ($Z_{eff}=2.5$)
($2x \langle \beta_{kin-e} \rangle$; 4.3%)

$\langle \beta_{beam} \rangle$; 1.5% (Cal. by FIT code)

Beam pressure effects on MHD; To be resolve

Relatively low n_e and low B_0 leads to large ratio of p_{beam} .

$\langle \beta_{dia} \rangle$; based on the diamagnetic measurement.

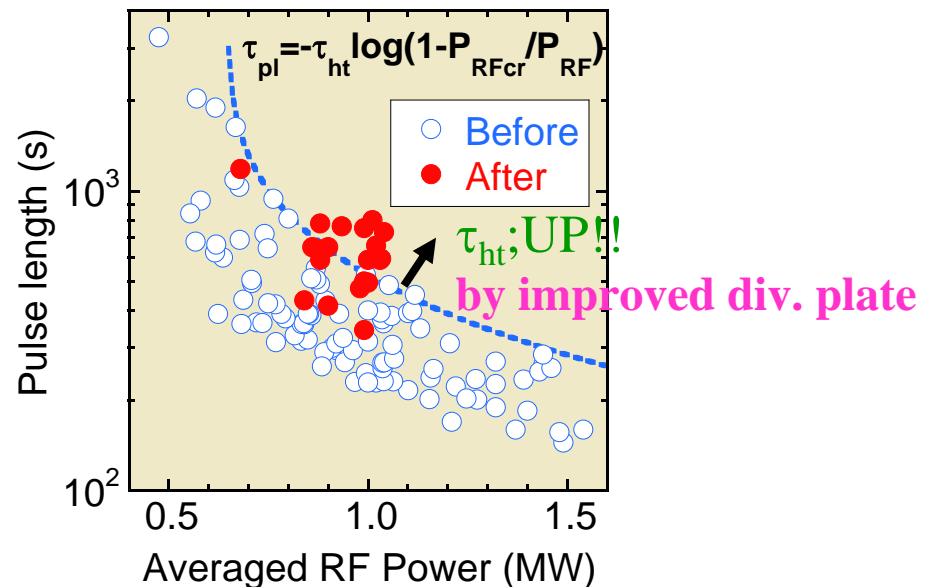
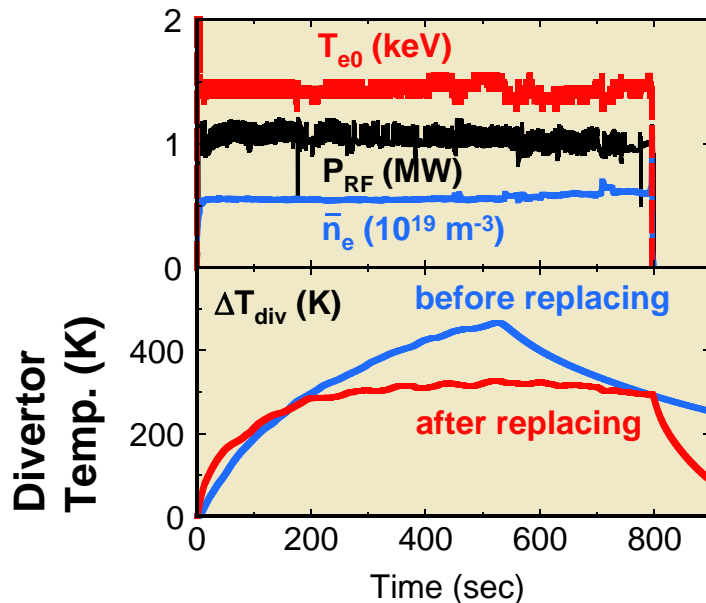
$\langle 2x \beta_{kin-e} \rangle$; based on the T_e and n_e profile measurements $Z_{eff}=1$ and $T_i=T_e$ are assumed.

(When $Z_{eff}=2.5$, $\langle \beta_{kin} \rangle \sim 3.6\%$ ($\beta_{perp} \sim 2.45$), $\langle \beta_{beam} \rangle_{perp} \sim 0.75\%$, $\langle \beta_{beam} \rangle_{ara} \sim 0.75\%$)

$\langle \beta_{beam} \rangle$; based on the calculation with Monte Carlo technique.

Demonstration of high input power and high heat load in Steady state

A scaling relation of the pulse length to the injected RF power was derived defining the critical temperature of divertor plates.



$P_{RF} = 1.1 \text{ MW}$ (ICH; 1 MW, ECH; 0.1 MW) for 800s

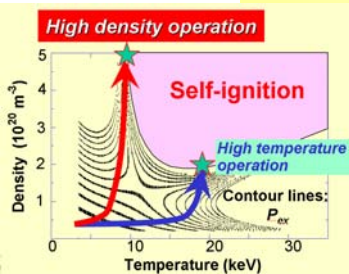
Divertor temperature is a key parameter of the observation of intensive spark.

Replacement of the improved divertor plates with good heat conductivity reduces the increment of divertor plate temperature.

Subjects on LHD Experiment to Reactor

Two reactor operation scenario

; High T /High n



LHD designed target
[Achievements]

Ion Temperature

T_{i0} 10 keV@ $2 \times 10^{19} \text{m}^{-3}$
[5.2 keV@ $1.6 \times 10^{19} \text{m}^{-3}$]

Electron Temperature

T_{e0} 10 keV@ $2 \times 10^{19} \text{m}^{-3}$
[10 keV @ $5 \times 10^{18} \text{m}^{-3}$]

Volume Averaged β

$\geq 5\%$ (1-2 T) [5.1% (0.425T)]

Steady State Operation

1 hour (3MW)
[54m28s(490 kW)1.6GJ,
800s(1.1MW)0.88GJ]

High Density

$[1.1 \times 10^{21} \text{m}^{-3}$ (with IDB)]

For high T scenario (conventional)

- # Reduction of neoclassical transport in low ν
(Demonstrate electron root under $T_i \sim T_e$)
- # High performance confinement in low ν and high β ,
under low beam pressure
(Confirm small effects of low-n MHD insta. &
resistive g turbulence in low S and high β)
 $\langle \beta \rangle > 4\%$ with $B_0 \sim 1\text{T}$ and/or $\langle \beta \rangle \sim 5\%$ with $B_0 > 0.8\text{T}$

For high n scenario (innovative)

- # Development of particle fueling method in the core
with high n and relatively high T repeatedly
- # Understandings of CDC mechanism to avoid it
(Study of ballooning, resistive MHD insta. and MHD
equil. limit and so on)
- # Study of transport property in stochastic regime

Under steady state operation

- # Study of impurity transport
(including development of He exhaust scenario)
- # Development of suppression method of heat load
to divertor

- 1. Demonstration of high ion temperature with confinement improvement similar to *Internal Transport Barrier (ITB)* accompanied by Impurity hole**
- 2. Achievement of high density $n_e(0) > 10^{21} \text{m}^{-3}$ with *Internal Diffusion Barrier (IDB)* and Extension of the high density operation regime with good energy confinement**
- 3. High beta $\langle \beta \rangle = 5\%$ is maintained in quasi-steady state and Demonstration of the high beta scenario consistent with high density reactor scenario**
- 4. Demonstration of high input power and high heat load in Steady state; 1.1MW for 800s**

LHD exp. related contributions (I/3, O/2, P/20)

I-11 M.Yoshinuma

Characteristic of an impurity hole in Large Helical Device

I-12 T. Morisaki

Topological Changes in Magnetic Flux Surfaces during IDB-SDC Discharge in LHD

I-21 T. Seki

Progress of Steady State Experiment in LHD

O-6 S.Murakami

Energetic ion confinement and lost ion distribution in heliotrons

O-7 A. Shimizu

The observation of potential fluctuation with 6 MeV Heavy Ion Beam Probe in LHD

P1-4 J. Miyazawa	Heating power dependence of the fusion triple product in high-density internal diffusion barrier plasmas in LHD
P1-9 S. Sakakibara	Effect of external magnetic perturbation on MHD characteristics in the Large Helical Device
P1-26 H.Yu. Zhou	Zeff Profile Analysis from Visible Bremsstrahlung Measurement under Different Density Profiles in LHD
P1-30 Y. Nobuta	Hydrogen Concentration and Crystal Structure of Carbon Films produced at the duct of Local Island Divertor in Large Helical Device
P1-32 E.A. Veshchev	Influence of Neutral Beam Injection Direction on Fast Ion Distribution Function in Large Helical Device (LHD)
P1-36 T. Ozaki	Comparison of neutral particle flux decay times on the NBI plasmas in Large Helical Device
P2-8 H. Takahashi	Development of 77 GHz-1 MW ECRH system for LHD
P2-10 Y. Yoshimura	2nd Harmonic ECCD experiment using 84 GHz EC-wave in LHD
P2-13 T. Oosako	Fast wave electron heating experiments focusing on competition between damping mechanisms on Large Helical Device
P2-17 G. Motojima	Spectroscopic diagnostics for spatial density distribution of plasmoid by pellet injection in Large Helical Device
P2-23 H. Chikaraishi	Voltage enhancement of the dc power supplies for dynamic current control of LHD superconducting coils
P2-28 M. Takeuchi	Development of a High Speed VUV Camera System for 2-Dimensional Imaging of Turbulent Structures in LHD
P2-31 S. Kubo	Collective Thomson Scattering Study using Gyrotron in LHD
P2-32 S. Muto	Observation of space and energy distributions of high-energy electrons produced in ECH plasmas of LHD
P2-33 M. Goto	Simultaneous measurement of electron and ion temperatures with heliumlike argon spectrum for LHD
P2-40 T. Yoshinaga	Fluctuation observation by the microwave imaging reflectometry in LHD
P2-41 D. Kuwahara	Development of 2-D Antenna Array for Microwave Imaging Reflectometry in LHD
P2-42 T. Oishi	Development of beam emission spectroscopy system for the measurement of density fluctuations in LHD
P2-43 C. Suzuki	Extension of the energy-resolved soft X-ray imaging system using two CCD cameras in LHD
P2-46 T. Minami	Development of in-situ Density Calibration for Thomson Scattering Measurement by Microwave Reflectometry on LHD